# **RSC Advances**



# **PAPER**

View Article Online
View Journal | View Issue



Cite this: RSC Adv., 2024, 14, 3024

# Effect of oxide impurities on the dissolution behavior of Th<sup>4+</sup>, Be<sup>2+</sup> and U<sup>4+</sup> in fluoride salts

Yubing Yan, <sup>Dab</sup> Yingjie Li, <sup>ab</sup> Haiying Fu, <sup>Da</sup> Yuan Qian, <sup>a</sup> Qingnuan Li, <sup>a</sup> Qiang Dou\* <sup>ab</sup> and Junxia Geng <sup>D\*ab</sup>

Oxides are one of the most important impurities in the fuel salt of molten salt reactors (MSRs), and excessive oxide impurities pose a risk to the safe operation of MSRs. This study focused on investigating the precipitation behavior between Th<sup>4+</sup>, U<sup>4+</sup>, and Be<sup>2+</sup> with O<sup>2-</sup> in the 2LiF-BeF<sub>2</sub> (FLiBe) eutectic salt system. The results showed that the solubility of UO<sub>2</sub> was  $5.52 \times 10^{-3}$  mol kg<sup>-1</sup>, and the solubility product ( $K_{sp}$ ) of UO<sub>2</sub> was  $6.14 \times 10^{-7}$  mol<sup>3</sup> kg<sup>-3</sup> in FLiBe salt at 650 °C. It was also found that the O<sup>2-</sup> ion would firstly react with U<sup>4+</sup> to form UO<sub>2</sub>, and then the excessive O<sup>2-</sup> would react with Be<sup>2+</sup> to generate BeO in the FLiBe system. Despite conducting the solubility experiment of ThO<sub>2</sub> and titration experiment of FLiBe-ThF<sub>4</sub>, the system failed to achieve the solubility and the  $K_{sp}$  of ThO<sub>2</sub>. The main reason for this was that O<sup>2-</sup> preferentially reacted with Be<sup>2+</sup> over Th<sup>4+</sup> to form precipitates, in other words, Be<sup>2+</sup> exerted a protective effect against Th<sup>4+</sup>. Above all, this work experimentally demonstrated that in the FLiBe system, O<sup>2-</sup> preferentially combines with U<sup>4+</sup> to form a precipitate, followed by Be<sup>2+</sup>, while Th<sup>4+</sup> is relatively inert.

Received 13th December 2023 Accepted 28th December 2023

DOI: 10.1039/d3ra08506f

rsc.li/rsc-advances

## Introduction

Reducing the use of fossil fuels seems to be an effective way to reduce CO<sub>2</sub> emissions and mitigate global warming, and many countries have chosen to develop sustainable nuclear power to partially replace traditional energy production. Consequently, significant efforts have been made to develop nuclear energy, and one of the current efforts is to develop the fourthgeneration advanced nuclear energy systems, such as molten salt reactors (MSRs). The characteristic of MSRs is the use of nuclear fuel in liquid form.2-4 The fissile material (UF4) and fertile material (ThF4) are dissolved in the molten carrier salt, and several alternative fuel carrier salts are being considered, but the leading candidate is 2LiF-BeF<sub>2</sub> (FLiBe).<sup>5-8</sup> Using liquid fuel will give MSRs an excellent advantage in performing continuous on-line fuel purification. On-line refueling significantly reduces the costs associated with fuel fabrication. More importantly, the ability to perform on-line fuel processing makes MSR suitable for the use of thorium.

In molten salt reactors, the purities are critical for controlling of chemical problems in the molten salt and mitigating corrosion. Among them, oxide impurities are a particularly important contaminant in this regard, because they can cause serious problems, such as fuel deposition and corrosion of structural materials.9-12 In addition to the impurities already

$$H_2O + 2F^- = 2HF + O^{2-}$$
 (1)

$$UF_4 + 2O^{2-} = UO_2 \downarrow + 4F^-$$
 (2)

For the safety of the molten salt reactor, it is necessary to strictly control the concentration of  $O^{2-}$  in the fuel salt. In addition, the molten salt oxide chemistry of this research will

present in the raw constituents of molten salt, partial oxide impurities are generated during reactor operation and maintenance. Water and oxygen are entrained in the gas phase of the reactor system, which are the major external sources of oxide impurities in MSRs; neutron irradiation of the fuel salt generates oxygen in the system during operation;13 and some oxides can penetrate into the MSRs fuel from passive layers formed on the surface of the structural materials.14 Although the oxide contamination in MSR is usually removed by sparging the molten salts with a mixture of H2 and HF to control the oxygen content of the molten salt within an acceptable range, 15-19 after the molten salt is loaded into the reactor, oxide impurities will still be introduced slowly in the manner described above. Previous studies have shown that UF4 in the fuel salt readily reacts with  $O^{2-}$  ions to form uranium oxide precipitates, as shown in eqn (2).20,21 The formation of uranium precipitates would reduce the concentration of U4+ and cause the loss of fuel, what's more, the large accumulation of UO<sub>2</sub> precipitates on the structural metal surface of the primary circuit would create the overheated areas in the reactor, posing a potential threat to the reactor operation.

<sup>&</sup>quot;Shanghai Institute of Applied Physics, Chinese Academy of Sciences, Shanghai, 201800, China. E-mail: gengjunxia@sinap.ac.cn; Tel: +86-21-39194027

buniversity of Chinese Academy of Sciences, Beijing 100049, China. E-mail: douqiang@sinap.ac.cn; Tel: +86-21-39190198

open the door to a deeper understanding of the precipitation and dissolution behavior of oxides in fluoride salts, which plays an important role in the chemical control of molten salt systems.

Studies of the dissolution and precipitation behaviors of UO<sub>2</sub> in fluoride salt have a long history, not least because of its importance in the safety of molten salt reactors. However, the existing studies showed a large scatter in the solubility product  $(K_{\rm sp})$  of  ${\rm UO}_2$ , and the desired data are often not available due to the inappropriate experimental conditions such as the temperature and composition of molten salt. Peng et al. 20,22 have studied the precipitation of UO2 in LiF-BeF2 and LiF-NaF-KF fluoride salt systems at 600 °C, using electrochemical methods. Their study showed that the  $K_{\rm sp}$  of  ${\rm UO_2}$  in the LiF-NaF-KF system was  $4.75 \times 10^{-6} \text{ mol}^3 \text{ kg}^{-3}$ , while in the LiF-BeF<sub>2</sub> system, it was  $1.67 \times 10^{-5} \text{ mol}^3 \text{ kg}^{-3}$ . There was an order of magnitude difference in the  $K_{\rm sp}$  of  $UO_2$  between the two systems. Oak Ridge National Laboratory (ORNL)23 studied the  $K_{\rm sp}$  of UO<sub>2</sub> in LiF–BeF<sub>2</sub>–ThF<sub>4</sub>–UF<sub>4</sub> at 500 °C, which was 2.60  $\times$ 10<sup>-7</sup> mol<sup>3</sup> kg<sup>-3</sup>. ORNL<sup>24</sup> has studied the system in detail and found that the  $K_{\rm sp}$  of UO<sub>2</sub> at 600 °C in the LiF-BeF<sub>2</sub>-ZrF<sub>4</sub> system was  $1.20 \times 10^{-5} \text{ mol}^3 \text{ kg}^{-3}$ . In LiF-BeF<sub>2</sub>-UF<sub>4</sub> with the addition of 5% ZrF<sub>4</sub>, Toth<sup>25</sup> found that Zr<sup>4+</sup> had a greater binding interaction for O<sup>2-</sup> than that of U<sup>4+</sup>. This finding has led to an increased interest in studying the interaction between Zr<sup>4+</sup> and O<sup>2-</sup>, as Zr<sup>4+</sup> can effectively integrate with O<sup>2-</sup>. This property, combined with its small neutron absorption cross-section (thermal neutron absorption cross-section of 0.18 bar), has even led several researchers to advocate ZrF4 as an ideal oxygen binding additive to prevent the precipitation of UO<sub>2</sub> in the fuel salt. Korenko<sup>21</sup> found that the introduction of oxide in the LiF-NaF-KF-UF<sub>4</sub>-ZrF<sub>4</sub> system can generate ZrO<sub>2</sub> precipitation, which effectively consumed the O2- in the molten salt and prevented the precipitation of UO2. Studies of the LiF-BeF2-ZrF<sub>4</sub>-UF<sub>4</sub> system by Peng<sup>26</sup> showed that ZrO<sub>2</sub> formed initially as an  $O^{2-}$  addition of less than 1 mol kg<sup>-1</sup>, with  $UO_2$  and  $ZrO_2$  coprecipitating at O<sup>2-</sup> additions greater than 1 mol kg<sup>-1</sup>. It implied that when oxide contamination exists in the melt containing both ZrF4 and UF4, a significant amount of ZrF4 could inhibit the UO2 formation. Later, Song and co-workers27 found that in the system of LiF-BeF2-ZrF4-UF4 system, when the molar ratio of Zr<sup>4+</sup> to U<sup>4+</sup> was greater than 4, only ZrO<sub>2</sub> precipitation formed after the quantitative addition of Li<sub>2</sub>O. Conversely, ZrO2 and UO2 co-precipitated when the molar ratio was less than 4.

Thorium has been acknowledged as a marvelous resource for its potential application as nuclear fuel, it has been considered as a possible supplement or even a replacement for uranium. Therefore, it is crucial to study the chemical behavior of Th<sup>4+</sup> in thorium-based molten salt reactors, as well as that of U<sup>4+</sup>. Chamelot *et al.*<sup>28</sup> reported that the addition of oxides to LiF-CaF<sub>2</sub>-ThF<sub>4</sub> produced the intermediate product ThOF<sub>2</sub>, and gradually formed the ThO<sub>2</sub> with more O<sup>2-</sup> added. Wang<sup>29</sup> used Raman spectroscopy to study the addition of Li<sub>2</sub>O to FLiBe/FLiNaK-ThF<sub>4</sub> and found that there was stabilized Th<sub>2</sub>OF<sub>10</sub><sup>4-</sup> anion with linear Th-O-Th geometry formed in both systems. Some related research on thorium utilization in molten salt

reactors has been published over the years, despite the numerous investigations on the products and structures of thorium compounds, less effort has been dedicated to the precipitation and dissolution behavior of Th<sup>4+</sup>.

The influence of  $O^{2-}$  ions on  $Th^{4+}$  and  $U^{4+}$  in the molten salt reactor has been proven to be significant. Researchers have attempted to establish an association between the precipitates of  $U^{4+}$ ,  $Th^{4+}$ , and  $O^{2-}$ . It is necessary to have an understanding about the solubility and solubility product ( $K_{\rm sp}$ ) of  $ThO_2$  and  $UO_2$ . Though a few studies have been performed for the solubility and  $K_{\rm sp}$  of  $UO_2$ , the results obtained are inconclusive. Furthermore, to our knowledge, there is limited research about solubility and  $K_{\rm sp}$  of  $ThO_2$  has been performed so far. Therefore, this study concentrates on the interaction between  $O^{2-}$  and  $U^{4+}$ ,  $Th^{4+}$ , as well as the precipitation and dissolution behavior of  $UO_2$  and  $ThO_2$  in the FLiBe system. This work aims to enhance knowledge of the oxide chemistry behavior in the FLiBe system.

# **Experiments**

#### Solubility experiments of UO2, ThO2

The UO2 and ThO2 (applied by North China Nuclear Fuel Components Co., Ltd) powders were compressed into tablets, as shown in Fig. 1(a) and (b), and positioned at the bottom of the crucible respectively. Next, 20 g of FLiBe salt was used to cover the tablets. To prevent any interference with sampling, a piece of nickel mesh was placed between the FLiBe molten salt and UO<sub>2</sub>/ThO<sub>2</sub> tablet to avoid powder diffusion. The UO<sub>2</sub> or ThO<sub>2</sub> was immersed in the FLiBe salt bath at 650 °C to create a saturated solution, which is illustrated in Fig. 2. Samples were taken hourly during the initial seven hours and subsequently every two hours. The samples were analyzed to determine the concentration of U4+ and Th4+ by ICP-OES, while the concentration of O2- by LECO oxygen analyzer and ion chromatography. Based on the concentrations of U<sup>4+</sup>/Th<sup>4+</sup> and O<sup>2-</sup> in salt samples, the solubility, as well as the solubility product  $(K_{sp})$  can be calculated.

#### Preparation of FLiBe-ThF4

In order to rapidly dissolve the  $ThF_4$  (supplied by Changchun Institute of Chemical Engineering, with a purity of 99.9%) into the fluoride salt, it is necessary to synthesize a molten mixture of LiF and  $ThF_4$  in advance. 10.2 g of  $ThF_4$  was mixed with 2.8 g of LiF and melted at a temperature of 700 °C to prepare LiF-

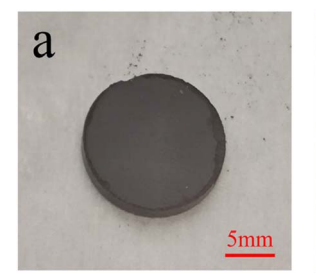




Fig. 1 (a) UO<sub>2</sub> after pressing; (b) ThO<sub>2</sub> after pressing.

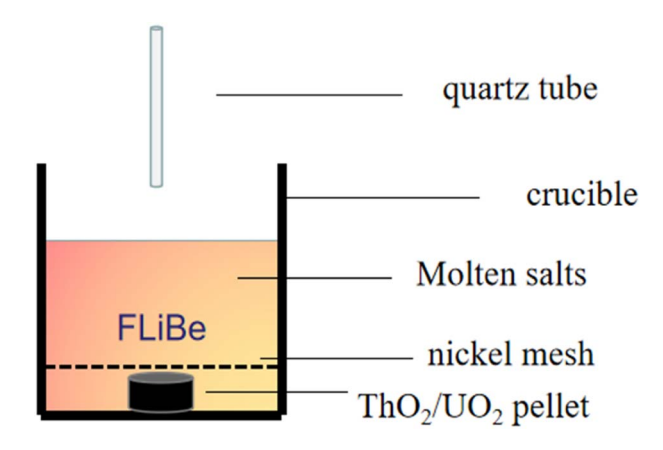


Fig. 2 Schematic diagram of solubility experiment of UO<sub>2</sub>/ThO<sub>2</sub>.

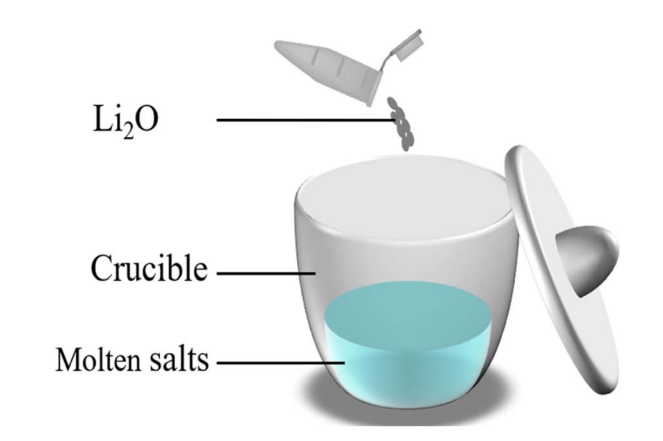


Fig. 3 Schematic diagram of FLiBe-UF<sub>4</sub>/ThF<sub>4</sub> titration experiment.

ThF<sub>4</sub>(FLiTh). The FLiTh was then mixed with FLiBe salt and heated to ensure that the ThF<sub>4</sub> uniformly dissolved into the FLiBe salt. The concentration of  ${\rm O}^{2-}$  within the resulting FLiBe–ThF<sub>4</sub> mixture was determined to be  $1.80 \times 10^{-2}$  mol kg<sup>-1</sup>.

#### Titration experiments of UF<sub>4</sub>/ThF<sub>4</sub> with Li<sub>2</sub>O in FLiBe

To investigate the reactions of  $\mathrm{U}^{4+}$  and  $\mathrm{Th}^{4+}$  with  $\mathrm{O}^{2-}$  in the FLiBe system and obtain the corresponding values of  $K_{\mathrm{sp}}$ , the titration experiments of  $\mathrm{UF_4/ThF_4}$  in FLiBe salt were carried out. In the titration experiment of FLiBe-UF<sub>4</sub>, 1 g of UF<sub>4</sub> (supplied by China National Nuclear Corporation, Baotou No. 202 Plant, 99.9% purity) was mixed with 19 g of FLiBe molten salt in a crucible; in the titration experiment of FLiBe-ThF<sub>4</sub>, 20 g of FLiBe-ThF<sub>4</sub> was used.  $\mathrm{O}^{2-}$  ions were added to the melts in the form of Li<sub>2</sub>O. After

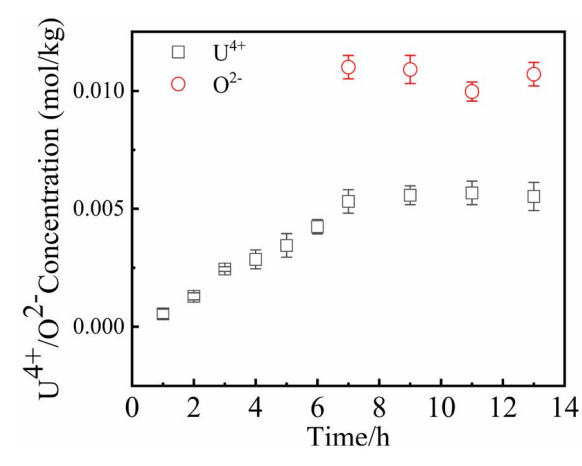


Fig. 4 Variation of U<sup>4+</sup> and O<sup>2-</sup> concentration with time at 650 °C.

the  ${\rm O^{2-}}$  was added, the salt mixture was stirred to ensure complete reaction of  ${\rm O^{2-}}$  ions with  ${\rm U^{4+}/Th^{4+}}$  ions in the salt (the schematic diagram is shown in Fig. 3). The temperature was maintained at 650 °C to allow the molten salt to settle, during the process, the supernatant was periodical extracted via a quartz tube for the concentration analysis of  ${\rm Th^{4+}}$ ,  ${\rm U^{4+}}$  and  ${\rm O^{2-}}$ .

#### Chemical analysis

The obtained samples were dissolved and diluted, and then the concentrations of cations (U<sup>4+</sup>, Th<sup>4+</sup>) in the molten salts were determined by ICP-OES (PerkinElmer Co., Ltd.). It was based on the premise that substances form a high-temperature plasma in a high-frequency electromagnetic field, so that the constituent elements of the compounds were generated into their excited states at high temperatures or by electric excitation, and that specific wavelengths of the electromagnetic spectral lines will be emitted when the elemental excited states were restored to the ground state, thus realizing qualitative or quantitative analyses of different samples.

The total concentration of O<sup>2-</sup> in the experiment was measured with the LECO oxygen detector (LECO RO600, LECO Co., Ltd.). The obtained sample was ground into powder and weighed precisely, with approximately 0.05 g sample being wrapped in a tin capsule and placed in a graphite crucible. During the test process, the molten salt sample quickly went through the feeding platform into the graphite crucible, and then switched the current to heat the crucible to 2700 °C in a short period. At the high temperature, the molten salt samples were melted, causing a reaction between the oxygen contained

Table 1 Oxygen content in oxygenated anions and FLiBe molten salt

Total oxygen content of FLiBe, mol kg <sup>-1</sup>	Oxygen content of oxygenated anions, mol $kg^{-1}$	Total oxygen content of oxygenated anions, mol $kg^{-1}$	${ m O}^{2-}$ content, mol ${ m kg}^{-1}$
$8.56 \times 10^{-3}$	$NO_3^- 1.56 \times 10^{-3}$ $PO_4^{3-} 2.13 \times 10^{-3}$ $SO_2^{2-} 3.56 \times 10^{-3}$	$7.25  imes 10^{-3}$	$1.31 \times 10^{-3}$

This article is licensed under a Creative Commons Attribution-NonCommercial 3.0 Unported Licence.

Open Access Article. Published on 18 sausio 2024. Downloaded on 2025-10-16 14:04:39

Paper

and carbon from the graphite crucible and generating CO and

CO<sub>2</sub> gases. The generated gases entered the infrared cell and were detected using infrared absorption. The computer assimilated the detection signals of CO and CO2 and subsequently calculated the total oxygen content value of the sample.

Weighed out about 0.1 g of sample into a PE bottle and added deionized water. The bottle was then put into an ultrasonic cleaner to extract the ions to be measured. Finally, the obtained liquid was quantitatively diluted and the oxygenated ions (NO<sub>3</sub><sup>-</sup>, PO<sub>4</sub><sup>3-</sup>, SO<sub>4</sub><sup>2-</sup>) in the molten salt were determined using an ion chromatograph (ICS-2100, Dionex Co., Ltd).

# Results and discussion

#### Content analysis of oxygen impurities in FLiBe salt

While the previous experiments and theoretical studies have focused on the oxygen impurity in fluoride salt, these results suggested that the oxygen impurities in the salt are composed of oxygen ions (O<sup>2-</sup>) and oxygenated anions (including NO<sub>3</sub><sup>-</sup>, PO<sub>4</sub><sup>3-</sup>, SO<sub>4</sub><sup>2-</sup> etc.).<sup>22,30</sup> During reactor operation and maintenance, the concentration of O<sup>2-</sup> ions within the fuel system would increase gradually, which was attributed to moisture and oxygen leaking into the reactor and the corrosion of the passive layers of the structural materials. Different from O2- ions, the oxygenated anions can be maintained at a relatively stable level, as oxygenated impurities were mainly introduced along with the carrier salt, LiF, BeF2 and UF4. etc.

The total oxygen content in the FLiBe molten salt was measured using a LECO oxygen analyzer. The oxygenated anions in molten salt were determined by ion chromatography. The practical O<sup>2-</sup> concentration ([O<sup>2-</sup>]) in molten fluorides was determined by subtracting the oxide concentration in oxygenated anions ([O]<sub>IC</sub>) from the total oxide concentration ([O]<sub>LECO</sub>), as shown in eqn (3). The measurement results of the total oxide concentration and the oxide concentration in oxygenated anions of FLiBe raw materials were listed in Table 1. The average total oxide concentration in the FLiBe molten salt was up to 8.56 imes10<sup>-3</sup> mol kg<sup>-1</sup>, as most of the oxygen and water contamination

products were removed by sparging the salt with a mixture of H<sub>2</sub> and HF. The main oxygenated anions were found to be NO<sub>3</sub><sup>-</sup>,  $PO_4^{3-}$ , and  $SO_4^{2-}$ . Based on the mass proportion of oxide in the oxygenated anion, the oxide concentrations in NO<sub>3</sub><sup>-</sup>, SO<sub>4</sub><sup>2-</sup>, and  $PO_4^{3-}$  were determined to have oxide concentrations of 1.56  $\times$  $10^{-3}$ ,  $2.13 \times 10^{-3}$ , and  $3.56 \times 10^{-3}$  mol kg<sup>-1</sup>, respectively. Thus, the resulting oxide concentrations in these three oxygenated anions were up to  $7.25 \times 10^{-3}$  mol kg<sup>-1</sup>, and the O<sup>2-</sup> content is then calculated to be  $1.31 \times 10^{-3}$  mol kg<sup>-1</sup> using eqn (3).

$$[O^{2-}] = [O]_{LECO} - [O]_{IC}$$
 (3)

#### Solubility of UO2 in FLiBe salt

Since UO<sub>2</sub> has been proven to be the main precipitate of U<sup>4+</sup> ions in the fuel system, 20 the key data of the solubility of UO2 in FLiBe salt is of great significance for controlling the oxide content of the fuel salt. In this study, the solubility of UO2 in FLiBe salt at a temperature of 650 °C was measured using the static dissolution method. UO2 tablet were used in these dissolution experiments. Fig. 4 shows the changes of U<sup>4+</sup> and O<sup>2-</sup> concentrations in FLiBe salt as a function of dissolution time, where U4+ content in molten salt was regarded as the amount of UO2 dissolved. It can be seen that the U4+ concentration kept increasing with an increase in dissolution time. Finally, as the dissolution time up to 7 hours, the  $[U^{4+}]$  reached a final plateau with a constant concentration, thus indicating that 7 h was the dissolution equilibrium time. Furthermore, the solubility of  $UO_2$  was calculated to be  $5.52 \times 10^{-3}$  mol kg<sup>-1</sup>. It should be noted that, as shown in Fig. 4, there are no significant fluctuations in the  $O^{2-}$  concentration profile as dissolution periods greater than 7 hours. The average oxygen content was approximately  $1.06 \times 10^{-2}$  mol kg<sup>-1</sup>, which is twice the U<sup>4+</sup> equilibrium concentration, consistent with the U/ O molar ratio in  $UO_2$ . Based on the concentration of  $O^{2-}$  and U<sup>4+</sup> in FLiBe salt, the solubility product of uranium and oxygen ions  $(K'_{sp})$  was determined to be 6.14  $\times$  10<sup>-7</sup> mol<sup>3</sup> kg<sup>-3</sup>, as shown in Table 2.

Table 2  $K_{sp}$  of  $UO_2$  obtained from solubility experiment

U <sup>4+</sup> , mol kg <sup>-1</sup>	Oxygen content, mol $kg^{-1}$	$K'_{\rm sp}$ , mol <sup>3</sup> kg <sup>-3</sup>	Average value
$5.31 \times 10^{-3}$	$1.11\times10^{-2}$	$6.54\times10^{-7}$	$6.14\times10^{-7}$
$5.57 \times 10^{-3}$	$1.09\times10^{-2}$	$6.07 \times 10^{-7}$	
$5.67 \times 10^{-3}$	$9.97 \times 10^{-3}$	$5.64 \times 10^{-7}$	
$5.52 \times 10^{-3}$	$1.07  imes 10^{-2}$	$6.32 \times 10^{-7}$	
	$5.31 \times 10^{-3}$ $5.57 \times 10^{-3}$ $5.67 \times 10^{-3}$	$0^{4+}$ , mol kg <sup>-1</sup> mol kg <sup>-1</sup> $0^{-2}$ $0^{-2}$ $0^{-2}$ $0^{-2}$ $0^{-2}$ $0^{-3}$ $0^{-2}$ $0^{-3}$ $0^{-2}$ $0^{-3}$ $0^{-3}$ $0^{-3}$ $0^{-3}$	0.00000000000000000000000000000000000

Table 3  $K_{\rm sp}$  of different ratios of UO<sub>2</sub> (initial U<sup>4+</sup> was 0.159 mol kg<sup>-1</sup>)

	Initial O <sup>2–</sup> , mol kg <sup>–1</sup>	Equilibrium $\mathrm{U}^{4+}$ , mol $\mathrm{kg}^{-1}$	Equilibrium $O^{2-}$ , mol $kg^{-1}$	$K_{\rm sp}$ , mol <sup>3</sup> kg <sup>-3</sup>	Average value
O1-U	0.157	$7.51  imes 10^{-2} \ 9.61  imes 10^{-3}$	$9.31  imes 10^{-3} \ 1.87  imes 10^{-2}$	$6.51 \times 10^{-6} \ 3.36 \times 10^{-6}$	$3.80\times10^{-6}$
O2-U O3-U	0.316 0.470	$9.61 \times 10^{-3}$ $3.34 \times 10^{-3}$	$1.87 \times 10$ $2.13 \times 10^{-2}$	$3.36 \times 10^{-6}$ $1.52 \times 10^{-6}$	

RSC Advances Paper

#### The titration of UF<sub>4</sub> with Li<sub>2</sub>O in molten FLiBe

Understanding the impact of O<sup>2-</sup> on the behavior of U<sup>4+</sup> in fluoride salt not only has fundamental interests but also is important for reactor operation and maintenance. The  $K_{\rm sp}$  of UO2 is one of the most important parameters in the oxide chemistry of fuel salt, indicating the interaction between U4+ and  $O^{2-}$  ions. This study aimed to investigate the  $K_{sp}$  of  $UO_2$ with different oxygen content by titrating UF<sub>4</sub> with Li<sub>2</sub>O in FLiBe salt. Three sets of titration experiments were conducted with Li<sub>2</sub>O/UF<sub>4</sub> ratios(molar ratio) of about 1:1, 1:2, and 1:3, which were called O1-U, O2-U and O3-U in this work, respectively. The equilibrium concentrations of U<sup>4+</sup> and O<sup>2-</sup> ions in molten FLiBe salt after each titration operation are given in Table 3. According to the data in Table 3, it was found that with an increase in the addition of Li<sub>2</sub>O from 0.157 mol kg<sup>-1</sup> to 0.470 mol kg<sup>-1</sup>, the equilibrium concentrations of U<sup>4+</sup> decreased sharply, while the equilibrium concentration of O<sup>2-</sup> accordingly increased from 9.31  $\times$  10<sup>-3</sup> mol kg<sup>-1</sup> to 2.13  $\times$ 10<sup>-2</sup> mol kg<sup>-1</sup>. Thus, based on the given data, the solubility product  $(K_{\rm sp})$  of U<sup>4+</sup> and O<sup>2-</sup> can be calculated to be  $3.80 \times 10^{-6}$  $\text{mol}^3 \text{ kg}^{-3}$ . This value was slightly greater than the  $K_{\text{sp}}$  obtained in the UO2 solubility experiment. This may be attributed to some un-deposited UO2 particles formed in the titration experiments, and these particles were picked up with the fluoride salt in the sampling process. The  $K_{\rm SD}$  of UO<sub>2</sub> obtained from the experiment is compared with that in the literature, the results are shown in Table 4.

As seen in Table 3, there was a clear difference between the initial addition value and the equilibrium value of U<sup>4+</sup> and O<sup>2-</sup> in the melts. The concentration variation of the two ions in these titration experiments is shown in Fig. 5. Inspected in more detail, it was revealed that the variation in concentration of the  $\Delta [U^{4+}]/\Delta [O^{2-}]$  ratio in the O1-U and O2-U experiments was about 1:2, consistent with the U/O molar ratio in UO2. Fig. 6 shows the photographs of solidified FLiBe-UF<sub>4</sub> salts after the titration experiments. It was evident that distinct reddishbrown precipitate layers appeared at the bottom of the salts. Meanwhile, with an increase in the addition of Li<sub>2</sub>O, the thickness of the precipitate layer increased, and the upper green molten salt gradually discolored. However, the results obtained in the O3-U experiment demonstrated that the  $\Delta [U^{4+}]/\Delta [O^{2-}]$ ratio was approximately 1:2.9, which was different from the U/ O molar ratio in UO<sub>2</sub>. It was found that the  $\Delta[U^{4+}]/\Delta[O^{2-}]$  ratio remained at 1:2.9 (shown in Table 5) upon repetition of the O3-U experiment.

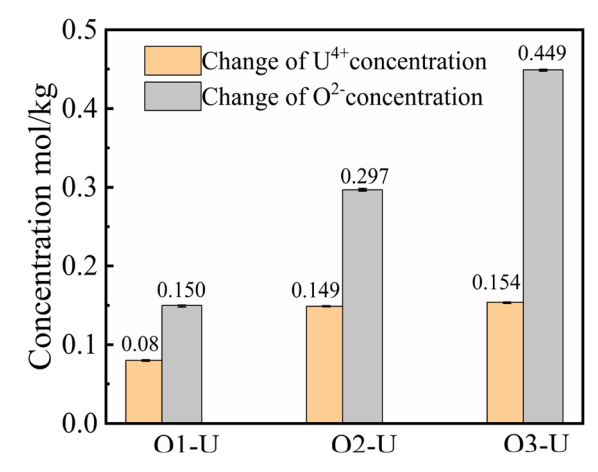


Fig. 5 Variation of  $\mathrm{U}^{4+}$ ,  $\mathrm{O}^{2-}$  concentrations for experiments with different ratios.

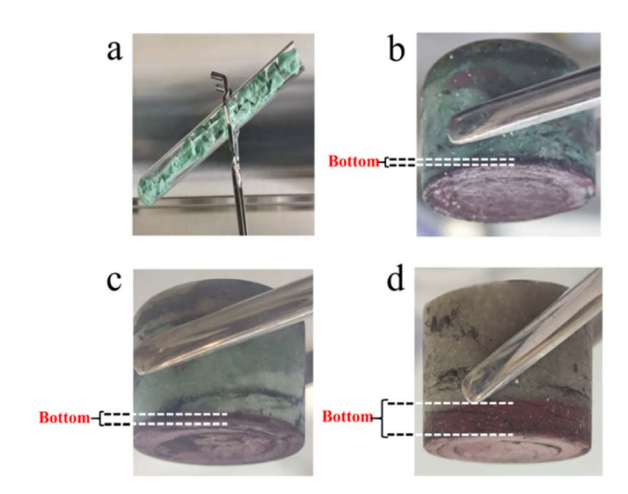


Fig. 6 (a) FLiBe-UF<sub>4</sub>; (b) molten salt of O1–U; (c) molten salt of O2–U; (d) molten salt of O3–U.

XRD analysis was performed on the reddish-brown precipitate after most of the FLiBe salt was removed (shown in Fig. 7). The diffraction peaks on the XRD pattern indicated that all the precipitate layers in these titration experiments contain a large amount of UO<sub>2</sub>. Later, these precipitates were analyzed by Raman spectrometer, and the analysis result (Fig. 8) showed that UO<sub>2</sub> was not the only generated precipitate in the O3-U experiment. Another insoluble oxide BeO<sup>31</sup> would form after

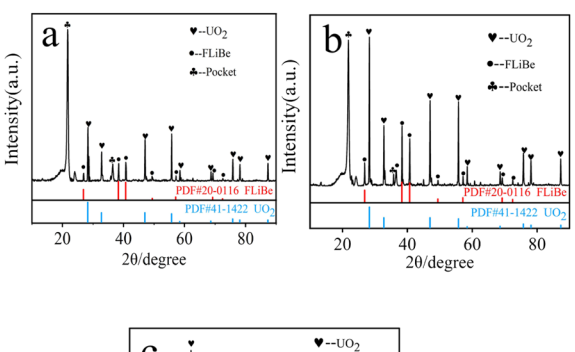
Table 4  $K_{sp}$  of UO<sub>2</sub> in different molten salt systems

Molten salt system	Temperature/°C	$K_{\rm sp}/{\rm mol^3~kg^{-3}}$	Experimental condition
LiF-BeF <sub>2</sub>	600	$1.67\times10^{-5}$	Titration experiment
LiF-NaF-KF	600	$4.75  imes 10^{-6}$	Titration experiment
LiF-BeF <sub>2</sub> -ThF <sub>4</sub> -UF <sub>4</sub>	500	$2.6 \times 10^{-7}$	Molten salt reactor
LiF-BeF <sub>2</sub> -ZrF4	600	$1.2\times 10^{-5}$	Molten salt reactor
LiF-BeF <sub>2</sub>	650	$6.14  imes 10^{-7}$	Solubility experiment
LiF-BeF <sub>2</sub>	650	$3.80 \times 10^{-6}$	Titration experiment

Paper

**Table 5** Concentration changes of  $\mathrm{U}^{4+}$  and  $\mathrm{O}^{2-}$  in the repeated experiment of O3–U

	Starting	Equilibrium	Variations	U <sup>4+</sup> :O <sup>2-</sup> percentage change
U <sup>4+</sup> mol kg <sup>-1</sup> O <sup>2-</sup> mol kg <sup>-1</sup>		$3.10 \times 10^{-3}$ $2.35 \times 10^{-2}$		1:2.9



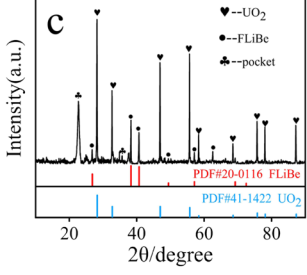


Fig. 7 (a) XRD analysis of the precipitate in O1–U; (b) XRD analysis of the precipitate in O2–U; (c) XRD analysis of the precipitate in O3–U.

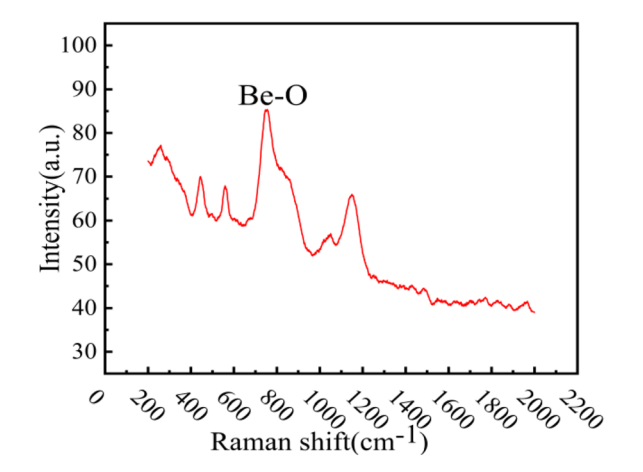


Fig. 8 Raman analysis of the precipitation in O3-U.

most  $U^{4+}$  ions were precipitated due to the successive addition of Li<sub>2</sub>O. Such a result may explain the distinct deviation of the  $\Delta$   $\left[U^{4+}\right]/\Delta\left[O^{2-}\right]$  ratio in the O3–U experiment.

#### Solubility of ThO2 in FLiBe salt

In MSRs using thorium, the deposition behavior of Th<sup>4+</sup> is worthy of attention. Previous research have indicated that the

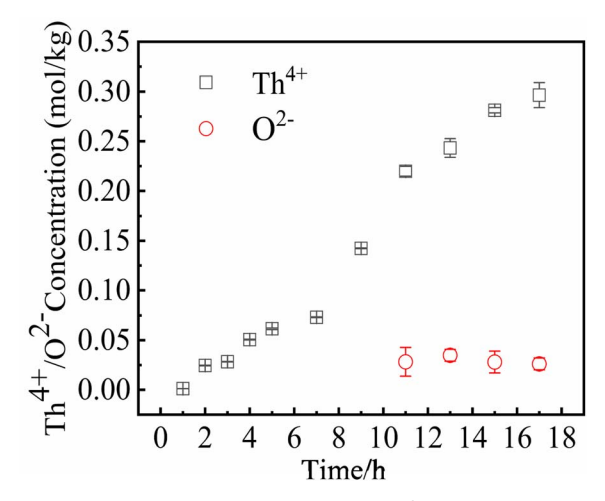


Fig. 9 Concentration changes of Th<sup>4+</sup> and O<sup>2-</sup> at 650 °C.

Th<sup>4+</sup> oxide precipitates in the form of ThO<sub>2</sub>.<sup>30</sup> In order to study the precipitation and dissolution behavior of ThO<sub>2</sub> in the FLiBe system, the solubility of ThO2 in molten FLiBe salt at 650 °C was studied by the static dissolution method. Fig. 9 presents the concentrations of Th4+ and O2- in the molten salt at different times. The concentration of Th $^{4+}$  increased from 1.24 imes $10^{-3}$  mol kg<sup>-1</sup> to 0.297 mol kg<sup>-1</sup>, and did not reach dissolution equilibrium after 18 hours. However, the [O<sup>2-</sup>] fluctuated within a small range of 0.03 mol kg<sup>-1</sup> after being dissolved for more than 10 hours, which was much less than the concentration of Th<sup>4+</sup>. The variation of concentrations was not only inconsistent with the Th/O molar ratio in ThO2 but also different from that of the UO<sub>2</sub> solubility experiment completely. Due to the continuous dissolution of Th4+ in FLiBe without reaching equilibrium during the experiment, the solubility and  $K_{\rm sp}$  of ThO<sub>2</sub> could not be determined.

To explore why ThO<sub>2</sub> fails to reach its dissolution equilibrium just as UO<sub>2</sub> does, XRD analysis was conducted on the insoluble substance at the bottom of molten salt after removing

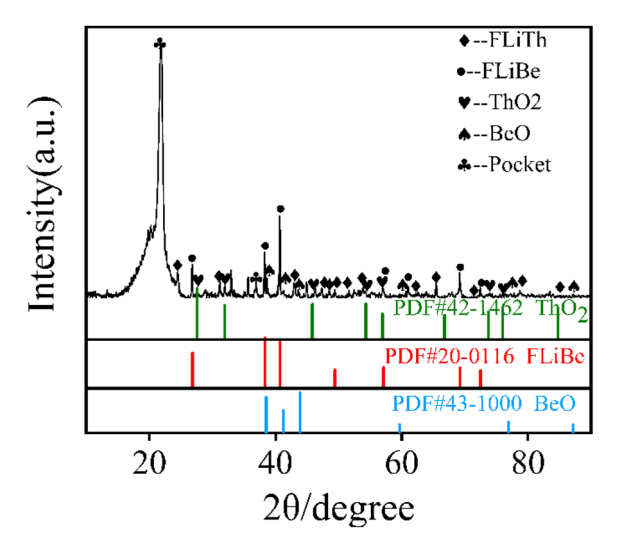


Fig. 10 Bottom precipitation XRD spectra of FLiBe-ThO<sub>2</sub> salt.

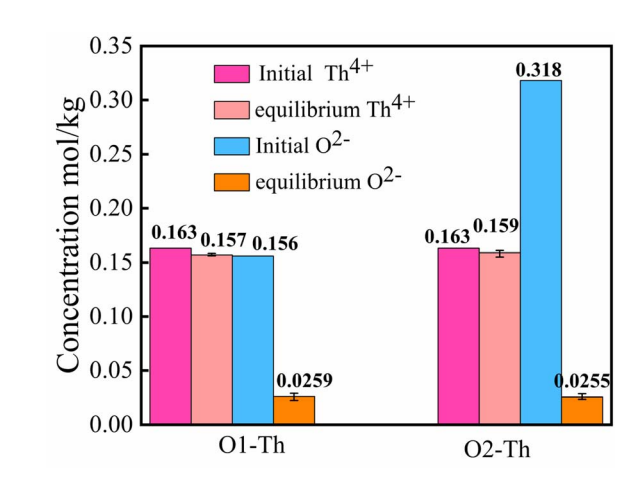


Fig. 11 Initial and equilibrium concentrations of Th<sup>4+</sup> and O<sup>2-</sup>.

Table 6 Concentrations of  $Th^{4+}$  ( $Th^{4+}$ :  $O^{2-} = 1:2$ )

	${ m Th}^{4+}$ , mol ${ m kg}^{-1}$
Upper part	0.160
Middle part	0.162
Lower part	0.157

the FLiBe salt by distillation. As shown in Fig. 10, it can be observed that BeO and  $ThO_2$  coexisted. It was speculated that the  $O^{2-}$  generated from dissolved  $ThO_2$  would react with  $Be^{2+}$ , which promoted the dissolution of  $ThO_2$ .

#### The titration of ThF<sub>4</sub> with Li<sub>2</sub>O in molten FLiBe

It failed to get the  $K_{\rm sp}$  of ThO<sub>2</sub> from the solubility experiment, which was extremely important to control the oxygen in molten salt, so the  $K_{\rm sp}$  of ThO<sub>2</sub> was intended to be measured using the same method as the UO<sub>2</sub> titration experiment mentioned above. Two sets of titration experiments were conducted with Li<sub>2</sub>O/ThF<sub>4</sub> ratio of about 1:1 and 1:2, denoted by O1-Th, O2-Th. Fig. 11 presents the initial and the equilibrium concentrations of Th<sup>4+</sup>, O<sup>2-</sup> in the molten salt, and shows a significant difference from the UO<sub>2</sub> titration experiment. As shown in this figure, with the addition of Li<sub>2</sub>O, there was no obvious change in the concentration of Th<sup>4+</sup>, while the [O<sup>2-</sup>] decreased unexpectedly. The result suggested that the introduction of O<sup>2-</sup> may react with other cations, leading to the dissolution behavior of Th<sup>4+</sup> to remain unaffected.

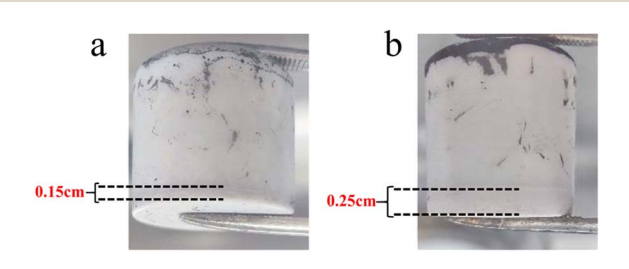


Fig. 12 (a) Molten salt of O1-Th; (b) molten salt of O2-Th.

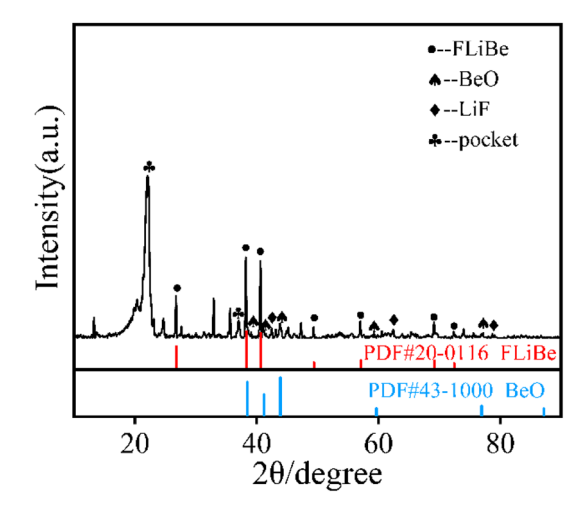


Fig. 13 XRD spectra of O2-Th bottom precipitation.

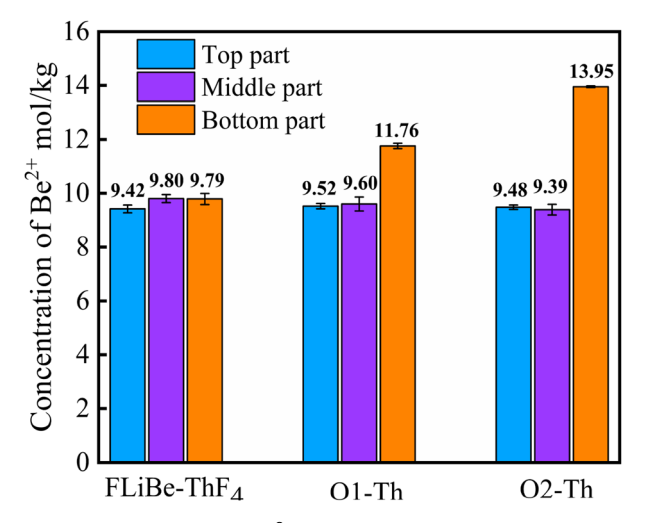


Fig. 14 Concentrations of Be<sup>2+</sup> in FLiBe-ThF<sub>4</sub>, O1-Th and O2-Th.

In order to determine whether the Th<sup>4+</sup> in molten salt reacted with O<sup>2-</sup>, the concentration of Th<sup>4+</sup> in different sections of the molten salt of O2-Th was analyzed, the relevant result was shown in Table 6. It was evident that the concentrations of Th<sup>4+</sup> in all three parts were similar, confirming that Th<sup>4+</sup> was uniformly distributed in the FLiBe salt. However, obvious precipitates were observed at the bottom of the salt (as shown in Fig. 12), and the thickness of the precipitate layer increased

**Table 7** Parallel measurement results of  $[Th^{4+}]$ ,  $[Be^{2+}]$ , and  $[O^{2-}]$  in FLiBe-ThF<sub>4</sub>-BeO titration experiments (initial  $Th^{4+}$ ,  $Be^{2+}$  were 0.163 and 9.67 mol  $kg^{-1}$ , respectively)

	Th <sup>4+</sup> , mol kg <sup>-1</sup>	Be <sup>2+</sup> , mol kg <sup>-1</sup>	O <sup>2-</sup> , mol kg <sup>-1</sup>
1	0.162	9.81	$1.57 \times 10^{-2}$
2	0.160	9.62	$1.75 \times 10^{-2}$
3	0.162	9.97	$1.89 \times 10^{-2}$
4	0.161	9.61	$1.89\times10^{-2}$

Paper RSC Advances

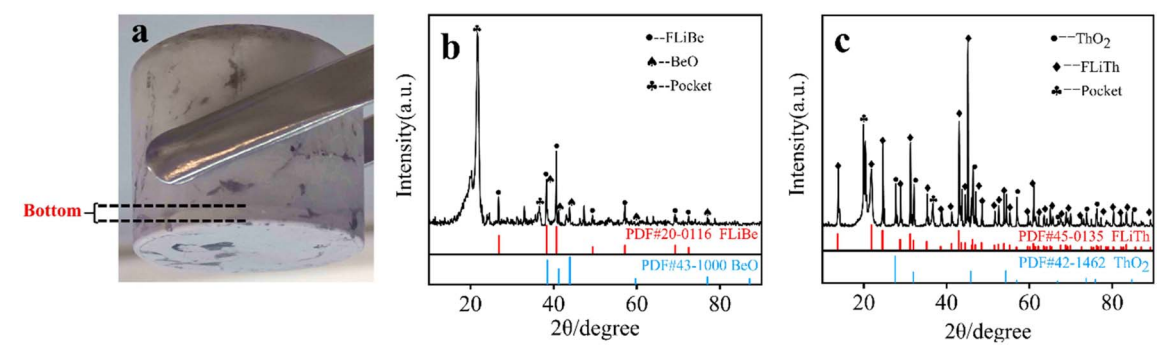


Fig. 15 (a) FLiBe-ThF<sub>4</sub>-BeO molten salt; (b) XRD spectrum of the precipitation of FLiBe-ThF<sub>4</sub>-BeO; (c) XRD spectrum of the precipitation of FLiTh-Li<sub>2</sub>O.

with the increase of  $O^{2-}$ . Subsequently, an XRD analysis was performed on the precipitate after most of FLiBe salt was removed (Fig. 13). The XRD pattern confirmed the presence of BeO but no ThO<sub>2</sub> in the precipitate.

Therefore, it is necessary to determine the concentration of  $Be^{2^+}$  in the molten salt. Fig. 14 illustrates the variation of  $[Be^{2^+}]$  at different sections within the molten salts of O1–Th, O2–Th, and FLiBe–ThF<sub>4</sub>. It can be seen that the  $[Be^{2^+}]$  remained relatively consistent across different positions in the FLiBe–ThF<sub>4</sub> molten salt. However, in the salts of O1–Th and O2–Th, the  $[Be^{2^+}]$  at the bottom was higher than that of the top and middle sections. Furthermore, the  $[Be^{2^+}]$  at the bottom of O2–Th was higher than that of O1–Th. These experimental findings suggested that the addition of  $O^{2^-}$  led to an enrichment of  $Be^{2^+}$  at the bottom, which could be attributed to the fact that  $O^{2^-}$  did not react with  $Th^{4^+}$  but with  $Be^{2^+}$  in the FLiBe system.

# The comparison of binding ability of $Th^{4+}$ , $Be^{2+}$ with $O^{2-}$ in fluoride salts

Based on the titration experiments results outlined above, two sets of experiments were specifically designed to investigate the interaction between Be<sup>2+</sup>, Th<sup>4+</sup> and  $O^{2-}$  in fluoride salts. To observe whether the Th<sup>4+</sup> has the ability to capture the  $O^{2-}$  from BeO, the titration experiment of ThF<sub>4</sub> in the FLiBe was conducted by adding BeO instead of Li<sub>2</sub>O. And to examine whether  $O^{2-}$  can combine with Th<sup>4+</sup> to generate ThO<sub>2</sub>, the titration experiment of ThF<sub>4</sub> with Li<sub>2</sub>O in FLiTh without Be<sup>2+</sup> was performed.

In the titration experiment of  $ThF_4$  with BeO in FLiBe, the ratio of  $BeO/ThF_4$  was set to be 1:2. The equilibrium  $[Th^{4+}]$  and  $[Be^{2+}]$  as well as the  $[O^{2-}]$  in the supernatant of the molten salt were listed in Table 7. It showed that there was no obvious change in the concentrations of  $Be^{2+}$ ,  $Th^{4+}$  and  $O^{2-}$ . However, Fig. 15(a) presents obvious precipitation at the bottom of the molten salt, and XRD characterization (the result shown in Fig. 15(b)) revealed that the precipitation was BeO. The experimental results confirmed that the BeO did not react with  $Th^{4+}$  in FLiBe molten salt, suggesting it is difficult for  $Th^{4+}$  to capture the  $O^{2-}$  in BeO.

In another titration experiment of ThF<sub>4</sub>, Li<sub>2</sub>O was directly added to FLiTh salt, and the precipitate obtained in this system

was characterized by XRD after the removal of the molten salt (shown in Fig. 15(c)). The XRD pattern clearly revealed the presence of ThO<sub>2</sub>, indicating that Th<sup>4+</sup> has the ability to react with O<sup>2-</sup> to form ThO<sub>2</sub> in the absence of Be<sup>2+</sup>.

Based on the solubility experiment of  $ThO_2$  and the titration experiment of  $ThF_4$  in FLiBe salt, it was clearly demonstrated that when  $O^{2-}$  was introduced into the FLiBe-ThF $_4$  salt, it preferentially reacted with  $Be^{2+}$  rather than  $Th^{4+}$ . This suggested that  $Be^{2+}$  had a protective effect on  $Th^{4+}$  in the fluoride salt system.

## Conclusions

To investigate the effect of  $\mathrm{O}^{2-}$  on the fuel salt of molten salt reactor, and provide a basis for understanding the chemical behavior of oxides in the fluoride salt system, this study focused on the solubility of  $\mathrm{UO}_2$  and  $\mathrm{ThO}_2$ , as well as the interaction behavior of  $\mathrm{O}^{2-}$  with  $\mathrm{U}^{4+}$ ,  $\mathrm{Th}^{4+}$ , and  $\mathrm{Be}^{2+}$  in the FLiBe system. The main findings are summarized as follows.

- (1) At a temperature of 650 °C, the solubility of UO $_2$  was 5.52  $\times$  10 $^{-3}$  mol kg $^{-1}$ , and the value of  $K_{\rm sp}$  was 6.14  $\times$  10 $^{-7}$  mol kg $^{-3}$ . When the added [O $^{2-}$ ] was less than twice of the [U $^{4+}$ ] in the FLiBe system, O $^{2-}$  would preferentially react with U $^{4+}$  to form UO $_2$  precipitate. As more O $^{2-}$  continued to be introduced, O $^{2-}$  would react with Be $^{2+}$  to generate BeO precipitate.
- (2) When  $O^{2-}$  was introduced into the FLiBe-ThF<sub>4</sub> system,  $O^{2-}$  would preferentially react with  $Be^{2+}$  rather than  $Th^{4+}$ , and only in the absence of  $Be^{2+}$ ,  $O^{2-}$  reacted with  $Th^{4+}$  to form  $ThO_2$ . In brief,  $O^{2-}$  introduced into the FLiBe molten salt at 650 °C would react firstly with  $U^{4+}$ , then with  $Be^{2+}$ , and finally with  $Th^{4+}$ .

Hence, when oxide impurities were introduced into the molten salt reactor fuel, it is important to take into account their impact on uranium to prevent the formation of  $UO_2$  precipitate. The current results indicated that the presence of a large number of  $U^{4+}$  and  $Be^{2+}$  played a certain protective role for  $Th^{4+}$ .

# **Author contributions**

Yubing Yan: methodology, investigation, writing – original draft, writing – review. Yingjie Li: data curation, investigation.

Haiying Fu: conceptualization, methodology. Yuan Qian: conceptualization. Qingnuan Li: conceptualization, validation. Junxia Geng: writing – review, supervision, validation. Qiang Dou: writing – review, validation, project administration, resources.

# Conflicts of interest

There are no conflicts to declare.

# Acknowledgements

This work was supported by the National Natural Science Foundation of China (No. 12175303 and U2267226), Xinjiang Uygur Autonomous Region Key R&D Task Special Project (No. 2022B01039).

#### References

- L. Mathieu, D. Heuer, R. Brissot, C. Garzenne, C. L. Brun,
   D. Lecarpentier, E. Liatard, A. Nuttin, E. Walle and
   J. Wilson, *Prog. Nucl. Energy*, 2006, 48, 664-679.
- 2 C. György and Sz. Czifrus, Prog. Nucl. Energy, 2016, 93, 306–317.
- 3 J. Serp, M. Allibert, S. Delpech, O. Feynberg, V. Ghetta, D. Heuer, D. Holcomb, V. Ignatiev, J. L. Kloosterman, L. Luzzi, R. Yoshioka and D. Zhimin, *Prog. Nucl. Energy*, 2014, 77, 308–319.
- 4 O. Benes and R. J. M. Konings, *J. Fluorine Chem.*, 2009, **130**, 22–29.
- 5 P. Souček, O. Beneš, B. Claux, E. Capelli, M. Ougier, V. Tyrpekl, J. F. Vigier and J. M. Konings, *J. Fluorine Chem.*, 2017, 200, 33–40.
- 6 C. Forsberg, Prog. Nucl. Energy, 2005, 47, 32-43.
- 7 A. Nuttin, D. Heuer, A. Billebaud, R. Brissot, C. Le Brun, E. Liatard, J. M. Loiseaux, L. Mathieu, O. Meplan and E. M. Lucotte, *Prog. Nucl. Energy*, 2005, 46, 77–99.
- 8 M. L. Tan, G. F. Zhu, Z. D. Zhang, Y. Zou, X. H. Yu, C. G. Yu, Y. Dai and R. Yan, *Nucl. Sci. Technol.*, 2022, 33, 5.
- H. Nishimura, T. Terai, T. Yoneoka, S. Tanaka, A. Sagara and
   O. Motojima, J. Nucl. Mater., 2000, 283–287, 1326–1331.
- 10 Y. L. Wang, Q. Wang, H. J. Liu and C. L. Zeng, *Corros. Sci.*, 2016, **103**, 268–282.
- 11 F. Y. Ouyang, C. H. Chang, B. C. You, T. K. Yeh and J. J. Kai, *J. Nucl. Mater.*, 2013, 437, 201–207.

- 12 K. M. Sankar and P. M. Singh, Corros. Sci., 2022, 206, 110473.
- 13 S. Q. Guo, J. S. Zhang, W. Wu and W. T. Zhou, *Prog. Mater. Sci.*, 2018, 97, 448–487.
- 14 N. J. Condon, S. Lopykinski, F. Carotti, K. E. Johnson and A. Kruizenga, *ACS Omega*, 2023, **8**, 29789–29793.
- 15 R. D. Scheele, A. M. Casella and B. K. McNamara, *Ind. Eng. Chem. Res.*, 2017, 56, 5505–5515.
- 16 D. A. Petti, G. R. Smolik, M. F. Simpson, J. P. Sharpe, R. A. Anderl, S. Fukada, Y. Hatano, M. Hara, Y. Oya, T. Terai, D. K. Sze and S. Tanaka, *Fusion Eng. Des.*, 2006, 81, 1439–1449.
- 17 A. L. Mathews and C. F. Baes Jr, *Inorg. Chem.*, 1968, 7, 373–382.
- 18 P. Calderoni, P. Sharpe, H. Nishimura and T. Terai, *J. Nucl. Mater.*, 2009, **386–388**, 1102–1106.
- 19 S. Delpech, C. Cabet, C. Slim and G. S. Picard, *Mater. Today*, 2010, 13, 34–41.
- 20 H. Peng, M. Shen, Y. Zuo, X. X. Tang, R. Tang and L. D. Xie, Electrochim. Acta, 2016, 222, 1528–1537.
- 21 M. Korenko, M. Straka, J. Uhlíř, L. Szatmáry, M. Ambrová and M. Šimurda, *J. Radioanal. Nucl. Chem.*, 2014, **302**, 549–554
- 22 H. Peng, W. Huang, L. D. Xie and Q. N. Li, J. Nucl. Mater., 2020, 531, 152004.
- 23 Molten-salt Reactor Program: the Development Status of Molten-Salt Breeder Reactors, ORNL-4812, 1972.
- 24 Molten-salt Reactor Program: Semiannual Progress Report for Period Ending, ORNL-3419, 1963.
- 25 L. Toth, U. Gat, G. Del Cul, S. Dai and D. Williams, *Review of ORNL's MSR technology and status*, Oak Ridge National Lab., 1996.
- 26 H. Peng, Y. L. Song, N. Ji, L. D. Xie, W. Huang and Y. Gong, RSC Adv., 2021, 31, 18708–18716.
- 27 Y. L. Song, M. Shen, S. F. Zhao, R. Tang, L. D. Xie and Y. Qian, *J. Electrochem. Soc.*, 2021, **168**, 036513.
- 28 P. Chamelot, L. Massot, L. Cassayre and P. Taxil, *Electrochim. Acta*, 2010, 55, 4758–4764.
- 29 C. Y. Wang, X. T. Chen and Y. Gong, *J. Phys. Chem.*, 2021, 125, 1640–1646.
- 30 M. Y. Xie, L. Li, Y. P. Ding and G. X. Zhang, *J. Nucl. Mater.*, 2017, **487**, 317–322.
- 31 S. M. Lee, Y. Jiang, J. Jung, J. H. Yum, E. S. Larsen, C. W. Bielawski, W. Wang, J. H. Ryoue, H. S. Kimf, H. Y. Chaf and J. Oh, *Appl. Surf. Sci.*, 2019, 469, 634–640.